Since January 2020 Elsevier has created a COVID-19 resource centre with free information in English and Mandarin on the novel coronavirus COVID-19. The COVID-19 resource centre is hosted on Elsevier Connect, the company's public news and information website.

Article

Immunity

Next-Generation Sequencing of T and B Cell Receptor Repertoires from COVID-19 Patients Showed Signatures Associated with Severity of Disease

Highlights

- Convergent B cell responses to SARS-CoV-2 epitopes are predominantly naive
- Shared T cell clusters emerge over disease course in recovering COVID-19 patients
- A receptor sequence repository from COVID-19 patients is established for public use

Authors

Christoph Schultheiß, Lisa Paschold, Donjete Simnica, ..., Sandra Ciesek, Marylyn Addo, Mascha Binder

Correspondence

mascha.binder@uk-halle.de

In Brief

It is unclear how immune responses to SARS-CoV-2 differ in patients with mild versus severe COVID-19 disease. Schultheiß et al. define specific immune receptor sequences associated with different disease courses and established an actively updated sequence repository for public use.

Schultheiß et al., 2020, Immunity *53*, 442–455
August 18, 2020
https://doi.org/10.1016/j.immuni.2020.06.024

CellPress

CellPress

Immunity

Article

Next-Generation Sequencing of T and B Cell Receptor Repertoires from COVID-19 Patients Showed Signatures Associated with Severity of Disease

Christoph Schultheiß,[1,11] Lisa Paschold,[1,11] Donjete Simnica,[1,11] Malte Mohme,[2] Edith Willscher,[1] Lisa von Wenserski,[1] Rebekka Scholz,[1] Imke Wieters,[3] Christine Dahlke,[4,5] Eva Tolosa,[6] Daniel G. Sedding,[7] Sandra Ciesek,[8,9,10] Marylyn Addo,[4,5] and Mascha Binder[1,12,*]

[1]Department of Internal Medicine IV, Oncology/Hematology, Martin-Luther-University Halle-Wittenberg, 06120 Halle (Saale), Germany
[2]Department of Neurosurgery, University Medical Center Hamburg-Eppendorf (UKE), 20246 Hamburg, Germany
[3]Infectious Diseases, Department of Internal Medicine II, University Hospital Frankfurt, 60596 Frankfurt am Main, Germany
[4]First Department of Medicine, Division of Infectious Diseases, University Medical Center Hamburg-Eppendorf, 20246 Hamburg, Germany
[5]Department for Clinical Immunology of Infectious Diseases, Bernhard Nocht Institute for Tropical Medicine, 20359 Hamburg, Germany
[6]Department of Immunology, University Medical Center Hamburg-Eppendorf, 20246 Hamburg, Germany
[7]Mid-German Heart Center, Department of Cardiology and Intensive Care Medicine, University Hospital, Martin Luther University Halle-Wittenberg, 06120 Halle (Saale), Germany
[8]Institute of Medical Virology, University Hospital, Goethe University Frankfurt, 60596 Frankfurt am Main, Germany
[9]Fraunhofer Institute for Molecular Biology and Applied Ecology (IME), Branch Translational Medicine und Pharmacology, 60596 Frankfurt am Main, Germany
[10]German Center for Infection Research (DZIF), External partner site Frankfurt, 60596 Frankfurt am Main, Germany
[11]These authors contributed equally
[12]Lead Contact
*Correspondence: mascha.binder@uk-halle.de
https://doi.org/10.1016/j.immuni.2020.06.024

SUMMARY

We profiled adaptive immunity in COVID-19 patients with active infection or after recovery and created a repository of currently >14 million B and T cell receptor (BCR and TCR) sequences from the blood of these patients. The B cell response showed converging IGHV3-driven BCR clusters closely associated with SARS-CoV-2 antibodies. Clonality and skewing of TCR repertoires were associated with interferon type I and III responses, early $CD4^+$ and $CD8^+$ T cell activation, and counterregulation by the co-receptors BTLA, Tim-3, PD-1, TIGIT, and CD73. Tfh, Th17-like, and nonconventional (but not classical antiviral) Th1 cell polarizations were induced. SARS-CoV-2-specific T cell responses were driven by TCR clusters shared between patients with a characteristic trajectory of clonotypes and traceability over the disease course. Our data provide fundamental insight into adaptive immunity to SARS-CoV-2 with the actively updated repository providing a resource for the scientific community urgently needed to inform therapeutic concepts and vaccine development.

INTRODUCTION

We are facing a pandemic of coronavirus disease 2019 (COVID-19) that is forcing us to live with the causative zoonotic severe acute respiratory syndrome coronavirus 2 (SARS-CoV-2), at least until a protective vaccine is developed. While there is no evidence for age-dependent differences of viral loads in COVID-19 patients, only a fraction of individuals exposed to the virus is infected and not all infected individuals develop the symptoms of COVID-19 (Wu and McGoogan, 2020). Similar to the two related viruses—SARS-CoV and the Middle East respiratory syndrome coronavirus (MERS-CoV)—SARS-CoV-2 harnesses the widely expressed angiotensin-converting enzyme 2 (ACE2) on the surface of host cells as an entry receptor (Hoffmann et al., 2020; Walls et al., 2020; Zhou et al., 2020). SARS-CoV-2 infection occurs in three stages: an asymptomatic incubation period (with the potential, however, of transmission to susceptible individuals), a mildly symptomatic period in some patients, and, in ~19% of confirmed cases, progression to a severely symptomatic state with 5% of critical disease courses (Rothe et al., 2020; Shi et al., 2020; Wang et al., 2020; Wu and McGoogan, 2020). Inferring from the pathophysiology of other coronaviruses, it is very likely that the capacity to mount a protective adaptive immune response plays a decisive role if viral propagation can be stopped early or if the virus will massively destroy tissues with high ACE2 expression, ultimately leading to a severe inflammatory state with relevant organ damage, specifically in the lungs and the kidneys (McKechnie and Blish, 2020; Puelles et al., 2020; Shi et al., 2020). Based on these assumptions, as long as no protective vaccine is available, antiviral and therapeutic approaches promoting adaptive immunity would seem to be the most promising early in the disease, whereas in later disease stages, it may be key to suppressing

inflammation to prevent tissue damage. However, there is only incomplete knowledge about the nature of T and B cell immune responses induced by SARS-CoV-2 and the factors determining the regulation of such responses and their persistence. This is especially true for non-hospitalized COVID-19 patients who achieved spontaneous viral clearance, thus providing a bottleneck resource for identifying successfully regulated anti-SARS-CoV-2 immune responses that are urgently needed to inform trial design and strategic vaccine development.

To close this gap, we performed a comprehensive immunological analysis to decode the adaptive immune response directed against the virus using next-generation immunosequencing flanked by antibody diagnostics, cytokine profiling, and flow cytometry in a cohort of hospitalized patients with active COVID-19 disease and a cohort that recovered from COVID-19 without medical intervention. The generated data reported here represents the basis for an actively updated repository (gateway.ireceptor.org; Study ID: IR-Binder-000001) opened for public scientific use that will allow researchers with different backgrounds to test their individual hypotheses on a growing dataset.

RESULTS

Cohorts and Laboratory Characteristics

We hypothesized that individuals with mild to moderate disease courses and early recovery would be a subset with effective immune control and persistent immune receptor signatures in post-infection blood, whereas patients with more severe or even fatal COVID-19 show an inflammatory reaction and fail to induce early protective immunity. Based on this assumption, we compiled a cohort of patients who recovered after COVID-19 (cohort 1, n = 19 patients, n = 20 samples) and a cohort of patients with active infection (cohort 2, n = 20 patients, n = 50 samples). Two patients overlapped in cohort 1 and 2 since samples from active disease as well as after recovery were available. Patients from cohort 1 with mild to moderate disease courses were generally younger (median age 34 versus 67 years in cohort 1 versus 2), were managed as outpatients, and the majority had no comorbidities. The majority of cohort 2 patients had comorbidities (18 of 20 with comorbidities linked to unfavorable COVID-19 outcome according to Wu et al. (2020a), all of the patients had to be hospitalized, and 12 of 20 patients were critically ill, with a need for mechanical ventilation or extracorporeal membrane oxygenation (ECMO). As a reference, we used an age-matched healthy donor (HD) cohort that tested negative for COVID-19 antibodies (n = 39). The characteristics of patient cohorts 1 and 2 are shown in Table S1 and the disease courses are shown in Figure 1. Human leukocyte antigen (HLA) typing results of the cohort are shown in Table S2.

Many patients with active (and mostly severe) COVID-19 showed leukocytosis, some with granulocytosis and pronounced T cell lymphopenia, while B lymphocyte counts were normal or even increased in the majority of patients (Figures 2A–2E). The $CD4^+$:$CD8^+$ T cell ratio was shifted toward $CD4^+$ T cells (Figure 2F), and regulatory T (Treg) cells were expanded in some patients (Figure 2G). Immunoglobulin G (IgG) and IgM concentrations were normal or decreased, but 5 of 13 evaluable patients had unexpectedly increased IgA amounts (Figure 2H).

A large proportion of all patients exposed to SARS-CoV-2 showed positivity for anti-SARS-CoV-2 IgA and IgG at some point, as measured by ELISA (32 of 37 patients; Figures 2I and 2J). An even higher percentage showed positivity by plasma neutralization assay at some point (35 of 37 patients; Figure 2K). Patients with active COVID-19 showed generally higher peak amounts of anti-SARS-CoV-2 antibodies than recovered patients, with relative IgG amounts of 6.3 compared to 2.1 (as measured by semi-quantitative ELISA) in a time span of 30–45 days after the first symptoms surfaced (Figure 2I). Of 70 time points analyzed by ELISA between a few days to 8 weeks after symptom onset, 48 were positive for IgA and IgG, 12 were negative for IgA and IgG, 6 were IgG negative but IgA positive, and only 3 were IgG positive but IgA negative (Figures 2I, 2J, and 2L). The neutralization assay detected antibodies more sensitively, with only 2 of the 70 time points resulting in negative numbers. Two of three patients with hematological malignancies developed delayed (patient 3, 4 weeks after COVID-19 contact) or only very weak and intermittent IgA antibody responses (patient 1), as tested by IgA and IgG ELISA, while the plasma neutralization assay was consistently positive, except for the first time point of patient 1. Patient 3 had been treated with rituximab ~6 months before infection with SARS-CoV-2, while patient 1 had undergone stem cell transplantation 7 months before infection and received immunosuppressive treatment for graft-versus-host disease, both treatments impairing B cell immune responses.

Persistent Cytokine Deregulation and Interferon Type I and III Responses in COVID-19 Patients

We reasoned that the previously reported cytokine storm in COVID-19 may be responsible for some of the blood count abnormalities of these patients (Mehta et al., 2020). IL-6 and IL-10, both involved in class switch recombination but also in T cell exhaustion, were significantly increased in the plasma of patients with active COVID-19, in line with previous data (Chen et al., 2020; Diao et al., 2020), while the recovered patients showed normal concentrations (Figure 3A). Also, plasma concentrations of B cell-activating factor (BAFF) were exclusively increased in active COVID-19 patients and exhibited a very unusual positive correlation with B cell counts, while a proliferation-inducing ligand (APRIL) was elevated only in the plasma of recovered patients (Figures 3A and S1). The antiviral cytokine pattern was compatible with an IFN type I and type III response, the latter persisting at increased levels during the recovery phase in COVID-19 (Figure 3B). COVID-19 had strong effects on the secretory variants of immune checkpoint molecules such as soluble Tim-3 (sTim-3), sLAG-3, sCD25, and sGalectin-9, which were normal in the recovered state, suggesting massive antiviral responses and counterregulation at the time point of active (and severe) disease (Figure 3C). All of the cytokines showing less profound alterations in COVID-19 are shown in Figure S2.

Early-Phase $CD4^+$ and $CD8^+$ T Cell Activation and Counterregulation with Shift toward T Follicular Helper, Th17, and Nonconventional Th1 Cell Responses in COVID-19

Based on the impact of SARS-CoV-2 on T cell numbers, the $CD4^+$:$CD8^+$ ratio, and secretory immune checkpoint molecules, we aimed to explore the functional state of T cells in COVID-19

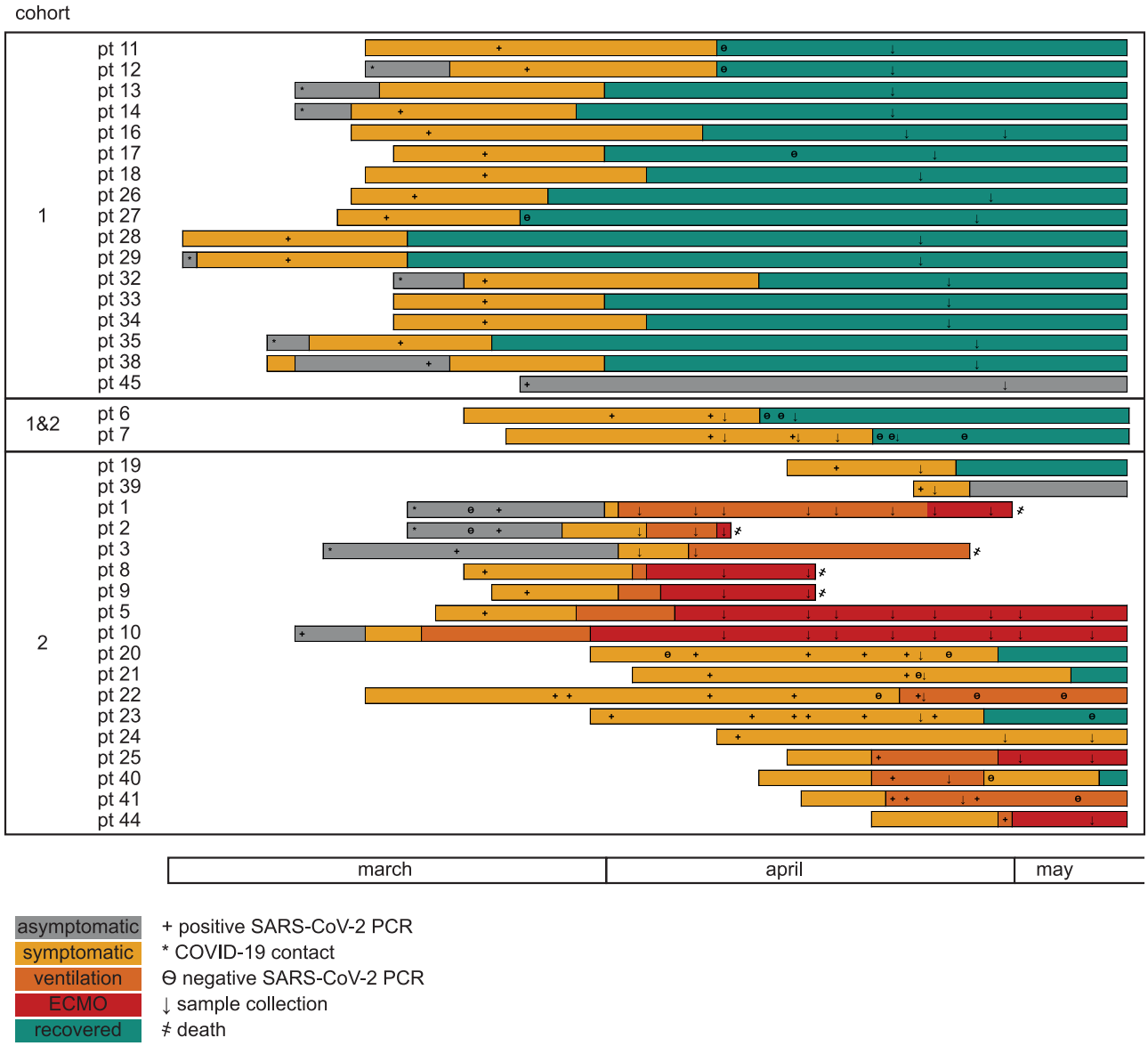

Figure 1. COVID-19 Disease Courses in Patients from Cohorts 1 and 2

Overview of COVID-19 disease course, intervention, and sample collection of patients infected with SARS-CoV-2 in cohort 1 (recovered) and 2 (active). pt, patient.

See also Tables S1 and S2.

by multiparametric flow cytometry. For this analysis, we used subjects with active disease at the date of sample collection, with samples acquired between 2 weeks and 1 month from symptom onset. We found 6 patients matching these selection criteria, 5 from cohort 2 and 1 from cohorts 1 and 2, with a median number of 23 days after symptom onset. Unsupervised cluster analysis clearly revealed 2 differentially abundant clusters (DACs) in the T cell compartment of COVID-19 patients (Figure 4A). As annotation of the markers indicates, both clusters contained cells expressing co-inhibitory receptors, namely BTLA (B and T lymphocyte attenuator), previously described to increase septic morbidity by inducing innate dysfunction (Shubin et al., 2012), and programmed cell death protein-1 (PD-1) and T cell immunoreceptor with Ig and immunoreceptor tyrosine-based inhibition motif domain (TIGIT). Further analysis of the expression of co-inhibitory receptors in each lymphocyte subpopulation confirmed that BTLA was strongly upregulated in both $CD4^+$ and $CD8^+$ T cells compared to controls (Figures 4B and 4C), indicating T cell activation and counterregulation in both subsets (Fuertes Marraco et al., 2015). While Tim-3 upregulation seemed to be a more important activation checkpoint for the $CD8^+$ subset, PD-1 upregulation was more pronounced on the $CD4^+$ subset, together with a strong downregulation of the metabolically active ecto-5′-nucleotidase CD73, which is also involved in the modulation of innate immune activation during viral immune response (Aeffner et al., 2015) (Figures 4B and

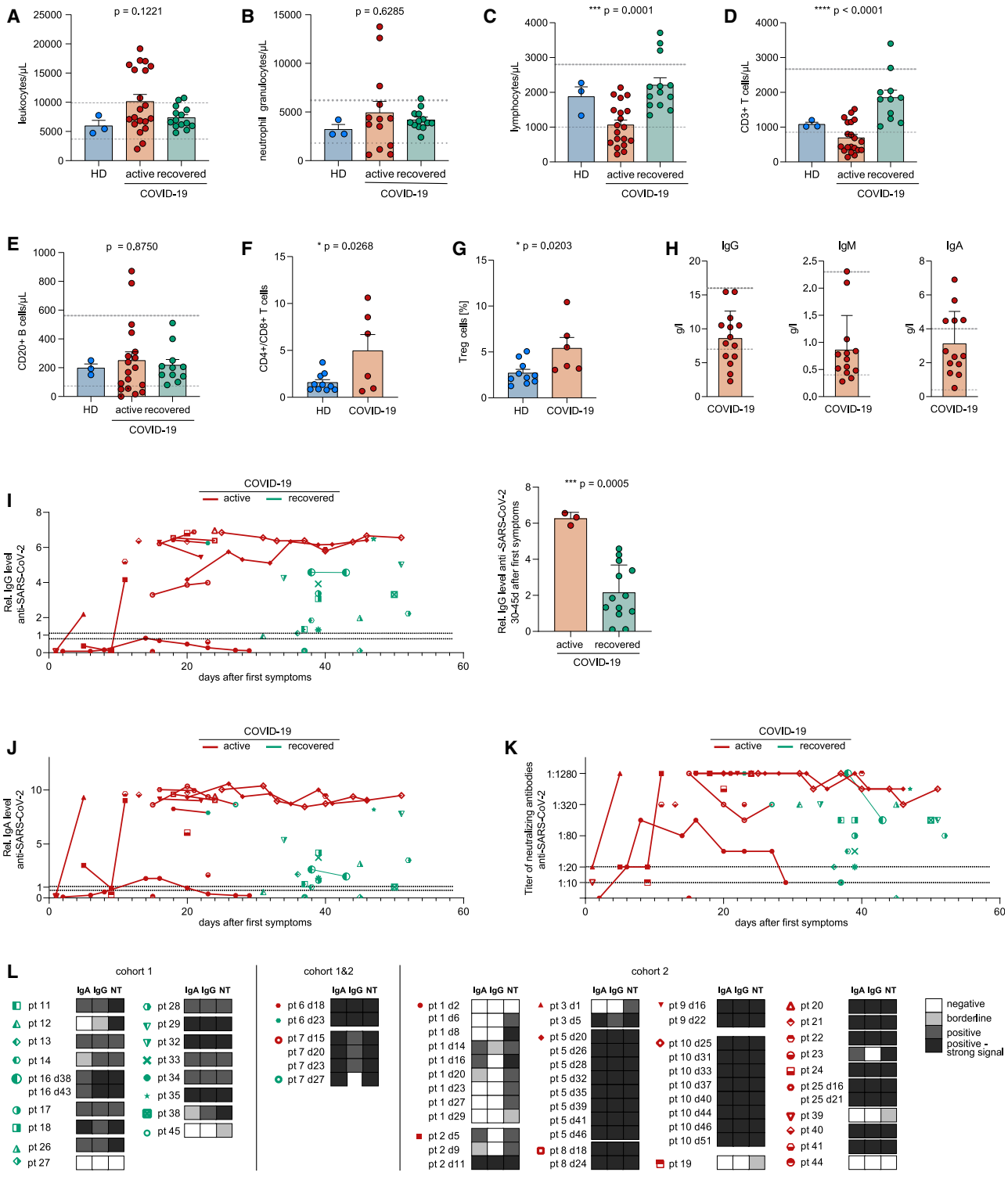

Figure 2. Basic Laboratory Characteristics of COVID-19 Cohorts

(A–E) Total number of leukocytes (A), granulocytes (B), lymphocytes (C), $CD3^+$ T cells (D), and $CD20^+$ B cells (E) per microliter of blood in HDs and COVID-19 cohorts 1 (recovered) and 2 (active). The gray dotted lines indicate the respective lower and upper limits of the reference range.

(F and G) Ratio of $CD4^+$:$CD8^+$ T cells (F) and percentage of regulatory T cells (G) in healthy donors (HDs) and patients with active COVID-19.

(H) Immunoglobulin (Ig) levels in patients with active COVID-19. Gray dotted lines indicate respective lower and upper limits of reference range.

(I and J) Relative levels of anti-SARS-CoV-2 IgG (I) and IgA (J). Black dotted lines indicate borderline range.

(legend continued on next page)

4C). Also, natural killer (NK) cells, significantly involved in antiviral responses, showed important signs of disinhibition by, for example, the downregulation of the inhibitory receptor TIGIT (Figures 4B and 4C). The proportions of naive and different stages of memory cells, in contrast, did not show any significant imbalance in COVID-19 patients (Figure 4E), supporting the finding that T cell responses are still in the early phase of immune activation in patients with active or severe COVID-19 infections. The dynamics of T helper (Th) subset differentiation, however, are already shifting, demonstrating profound T follicular helper (Tfh) and Th17-like, and to some degree nonconventional, ($CCR6^+$ $CCR4^+$) Th1 (Th1*) polarization (Becattini et al., 2015), while the classical antiviral Th1 axis was not induced (Sallusto, 2016) (Figure 4D). In contrast to the classical Th1 cells, the recently described Th1* cells express CD161 and interleukin-1 receptor type I (IL-1RI) typical for Th17, but not classical Th1, cells. However, despite sharing these features with Th17 cells, Th1* cells do not produce IL-17 (Sallusto, 2016). Dimensionality reduction of immune profiling data on activation and co-inhibitory receptors for individual patients show the profound global differences between COVID-19 patients and HDs (Figure S3).

Creation of a Repository for B and T Cell Receptor Sequences from COVID-19 Patients

Our analysis of blood B and T cell compartments and antibody repertoires confirmed some of the previously reported and revealed new aspects of COVID-19 immune responses, suggesting that SARS-CoV-2 substantially affects adaptive immunity and immune cell architecture and function. Using in-depth sequence analyses of B and T cell repertoires in our 2 informative cohorts, we hypothesized that we could reveal the nature of protective versus detrimental B and T cell responses. This may be used as a prognostic biomarker in patients and is critically needed to develop monoclonal antibodies to SARS-CoV-2, but also to determine the optimal T cell engagement strategy for vaccine development. For this purpose, we created a COVID-19 BCR and TCR sequence repository in response to the COVID-19 pandemic that is continuously fed with new annotated sequence data (details on data deposition are illustrated in Figure S4; gateway.ireceptor.org; Study ID: IR-Binder-000001). At the time of manuscript submission, the repository contained sequences from a total of 37 patients, including 69 time points, and overall >6.2 million BCR and >8.3 million TCR sequences that were retrieved from this repository for the analyses presented here. Sequencing details and depths of BCR and TCR repertoires are shown in Table S3.

Convergence of B Cell Responses toward IGHV3-Containing Rearrangements without Somatic Hypermutation in COVID-19

Global Ig heavy-chain gene (IGH) metrics showed slightly more diverse and richer repertoires in COVID-19 patients, an effect that was more pronounced in the recovered cases of cohort 1 (Figure 5A). Overall, only very slight increases in IGH somatic hypermutation as a proxy for germinal center reactions were discernible in repertoires from COVID-19 patients as compared to HDs (Figure 5B). It is noteworthy that there was a rather broad range of somatic hypermutations across individuals. To study a potential clinical significance associated with this, we compared the rates of somatically mutated BCRs per patient in critically ill individuals who had required mechanical ventilation or ECMO with those of hospitalized individuals who did not require any ventilation support in the course of their disease. This analysis showed that high somatic hypermutation (corresponding to a low percentage of naive B cells) was a pattern associated with a more severe clinical picture (Figure 5B). Notably, BCRs with high somatic hypermutation did not display evidence for clonal expansion as compared to BCRs without.

Next, we examined our dataset for conserved sequence features indicating the shared imprints of a convergent B cell response in COVID-19 patients, thus reducing repertoire complexity for the identification of potential BCRs corresponding to selected antibodies targeting SARS-CoV-2. To achieve this, we retrieved the 50 most frequent BCR clonotypes from a subset of 13 randomly chosen anti-SARS-CoV-2 positive repertoires of both cohorts (Figures 2I–2K), as well as 6 control COVID-19 repertoires without detectable anti-SARS-CoV-2 IgG or IgA antibody titers and subjected this subset of 19 repertoires to phylogenetic sequence analysis. Only B cell clusters derived from at least 10 unique BCR clonotypes and at least 4 different COVID-19 patients were considered to be potential sources of SARS-CoV-2 targeting antibodies. To estimate the specificity of our clustering approach, we used a positive and negative control cohort. The positive control consisted of HDs immunized with recombinant recombinant vesicular stomatitis virus-vectored Ebola vaccine (rVZV-EBOV, the recently licensed Ebola vaccine [Ervebo]) who developed rVZV-EBOV-specific antibodies at day 28 after vaccination (cohort characteristics and sequencing depths are shown in Table S4). These 13 BCR repertoires were aligned with 5 BCR repertoires from individuals who did not develop rVZV-EBOV-specific antibodies at day 28 after vaccination. As a negative control, we used 13 and 6 randomly chosen BCR repertoires from HDs that were studied using the same algorithm. The phylogenetic analysis revealed 15 clusters of related BCR sequences in antibody-positive COVID-19 repertoires and 11 clusters after rVZV-EBOV vaccination, while 5 clusters were generated from the 2 randomly chosen sets of unchallenged HD repertoires. The COVID-19 clusters spanned different individuals that apparently had, independently of one another, engaged in very similar B cell responses characterized by the preferential usage of Ig heavy chain variable region 3 (IGHV3) subfamily genes, mostly rearranged with Ig heavy chain joining region 4 (IGHJ4) or IGHJ6 gene segments. In contrast, the vaccine-specific clusters from the Ebola cohort exhibited a more scattered usage of IGHV genes. Of note, the majority of COVID-19-specific IGHV3 BCR clusters contained unmutated BCR sequences (Figure 5C). This was in line with our metrics data, suggesting that patients with more effective

(K) Neutralizing antibodies against infectious SARS-CoV-2 isolate were analyzed. Analysis was started with a 1:10 dilution. Seropositivity is defined by a titer $\geq$1:20.

(L) Heatmap of results from (I)–(K). NT, neutralizing anti-SARS-CoV-2 antibodies. The error bars indicate mean ± SDs. Statistical analysis: 2-sided unpaired t-test (2 groups), ordinary 1-way ANOVA (3 groups).

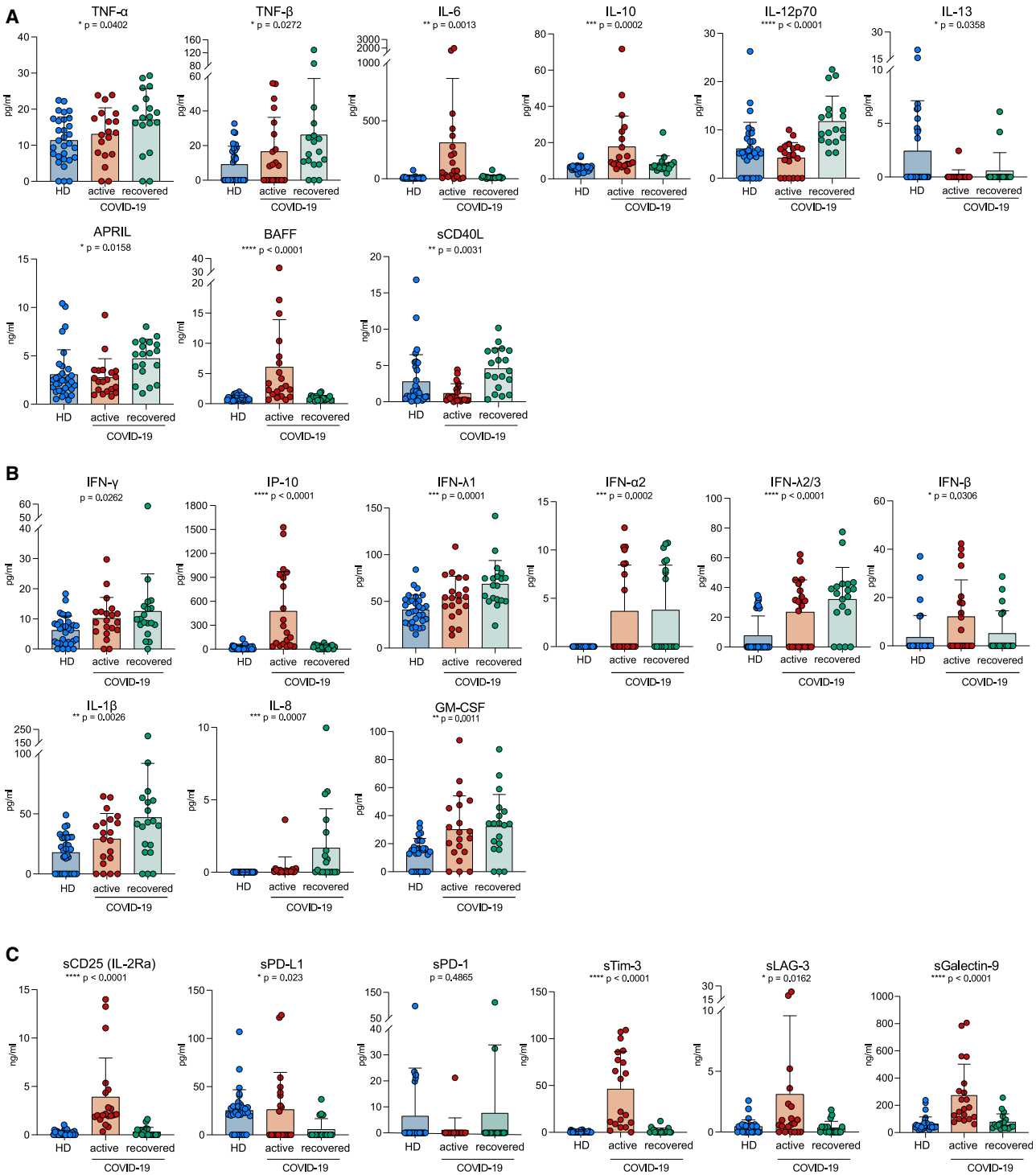

Figure 3. Profiling of Soluble Factors in COVID-19 Patients Shows Persistent Cytokine Deregulation and Interferon (IFN) I and III Responses

Mean plasma levels of cytokines key to B cell function (A) and viral response (B), as well as soluble immune checkpoints (C) in patients with active disease (n = 20) or after recovery (n = 19) compared to HDs (n = 32). All samples were measured at least in duplicates. Additional data are included in Figure S2. The error bars indicate means ± SDs. Statistical analysis: ordinary 1-way ANOVA.

See also Figures S1 and S2.

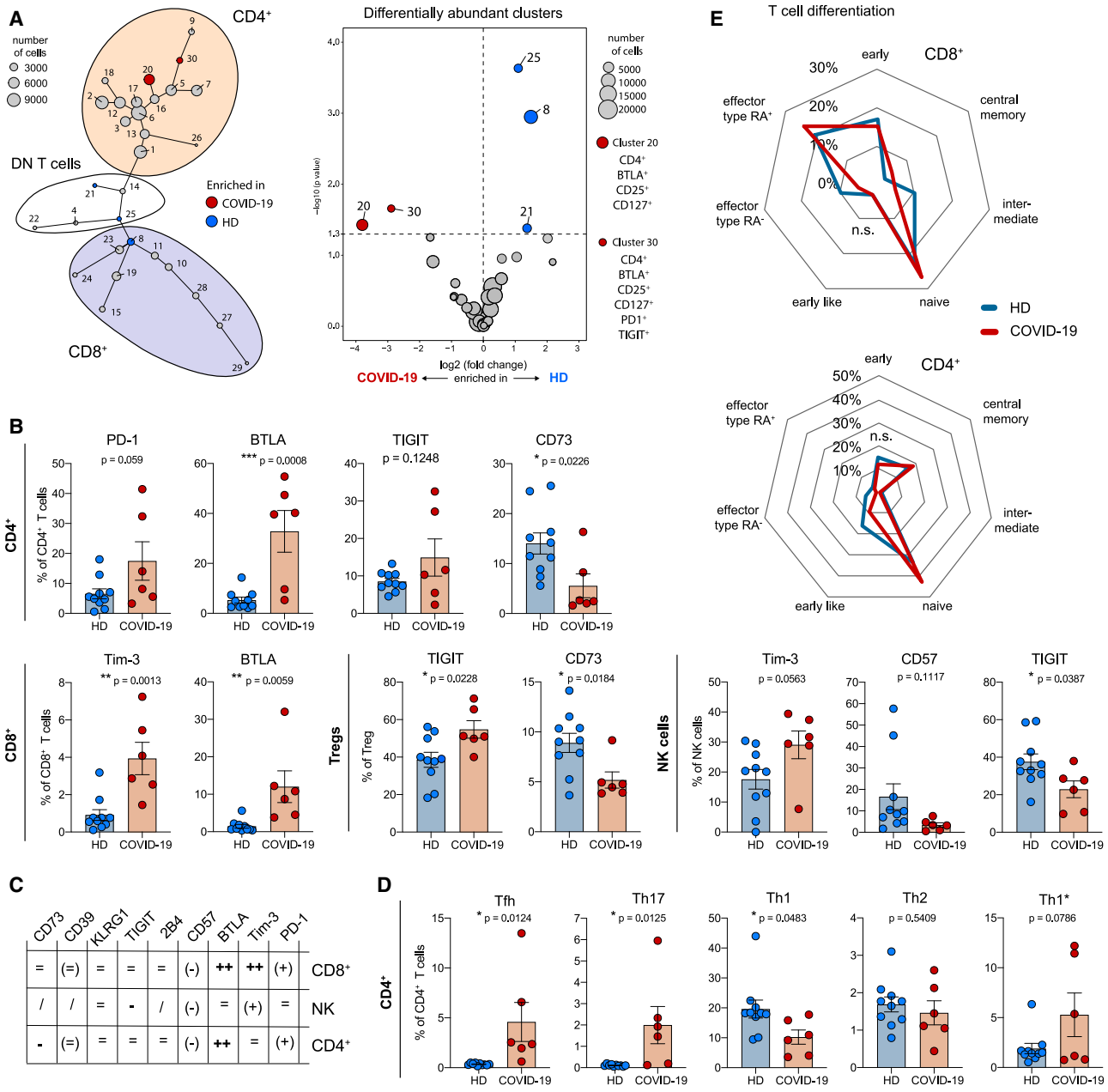

Figure 4. T Cells from COVID-19 Patients Show Early-Phase CD4⁺/CD8⁺ Activation and Helper Cell Polarization toward Tfh, Th17, and Th1 Responses

(A) Unbiased analysis of flow cytometry data using SPADEVizR trees shows significant enrichment of differentially abundant clusters (DACs) in active COVID-19 patients and HDs.

(B) Results of manual flow cytometry analysis of T and NK cell surface markers depict increased expression of inhibitory markers and ectoenzymes. Values are represented as the percentage of the respective cell population.

(C) Comparison of T and NK cell activation and exhaustion markers between COVID-19 patients and HDs. ++, Significantly increased in COVID-19; (+), increased in COVID-19; =, similar in COVID-19 and HDs; (-) decreased in COVID-19, -, significantly decreased in COVID-19; /, not applicable. Additional data are included in Figure S3.

(D) Th cell subsets in HDs and COVID-19 patients. Values are represented as the percentage of CD4⁺ T cells, respectively. Tfh, T follicular helper cells. Th1*, non-classical Th1 cells.

(E) Differentiation and maturation profiles of CD8⁺ and CD4⁺ T cells. The error bars indicate mean ± SEMs. Statistical test: 2-sided unpaired t test.

See also Figure S3.

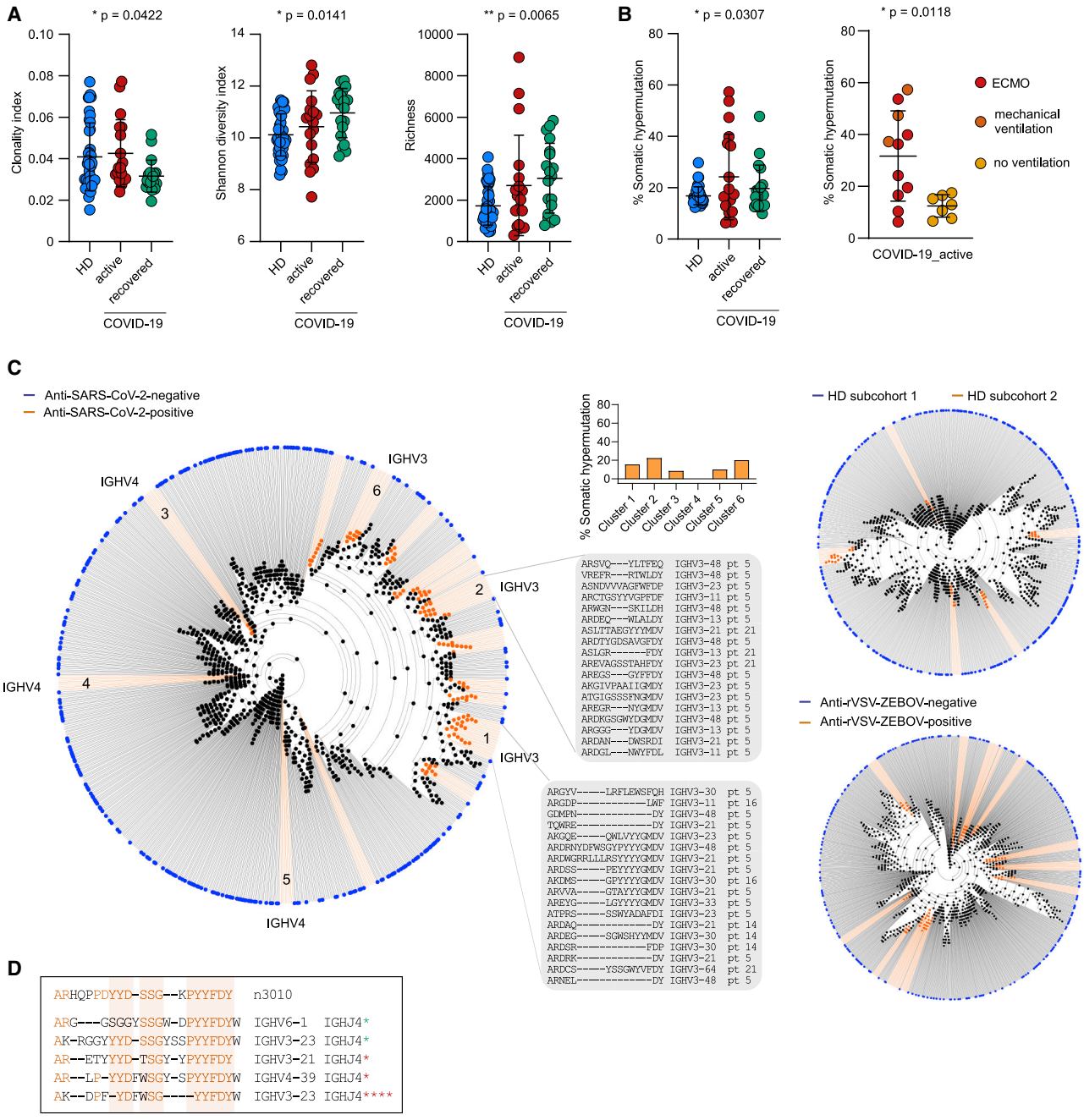

Figure 5. B Cell Repertoire Analysis from Living COVID-19 Sequence Repository Shows BCR Rearrangements Converging toward IGHV3 Usage with Low Somatic Hypermutation and Homology with Antibody Sequence Selected against the SARS-VoV-2 S1 Antigen

(A) Peripheral blood IGH repertoire metrics of HDs and patients with active COVID-19 and after recovery.

(B) Percentage of peripheral blood BCRs with somatic hypermutation in HDs and patients with active COVID-19 and after recovery. IGH hypermutation in patients with active COVID-19, depending on ventilation status and severity of disease. ECMO, extracorporeal membrane oxygenation. The error bars indicate mean ± SDs. Ordinary 1-way ANOVA (3 groups) or 2-sided unpaired t-test (2 groups) were used to study the differences between cohorts.

(C) B cell repertoire-wide phylogenetic tree analysis of SARS-CoV-2 ELISA-positive (n = 13) versus -negative (n = 6) samples (left panel), HDs (upper right panel), and an Ebola vaccination cohort (lower right panel). The top 50 clones per IGH repertoire were used for the analysis.

(D) Sequence alignment between BCR sequences derived from IGH repertoires of COVID-19 patients from our cohorts, with a SARS-CoV-2 neutralizing single-domain antibody (n3010) recently isolated by Wu et al. (2020c). The asterisk indicates the number of patients.

See also Figure S4 and Tables S3, S4, and S5.

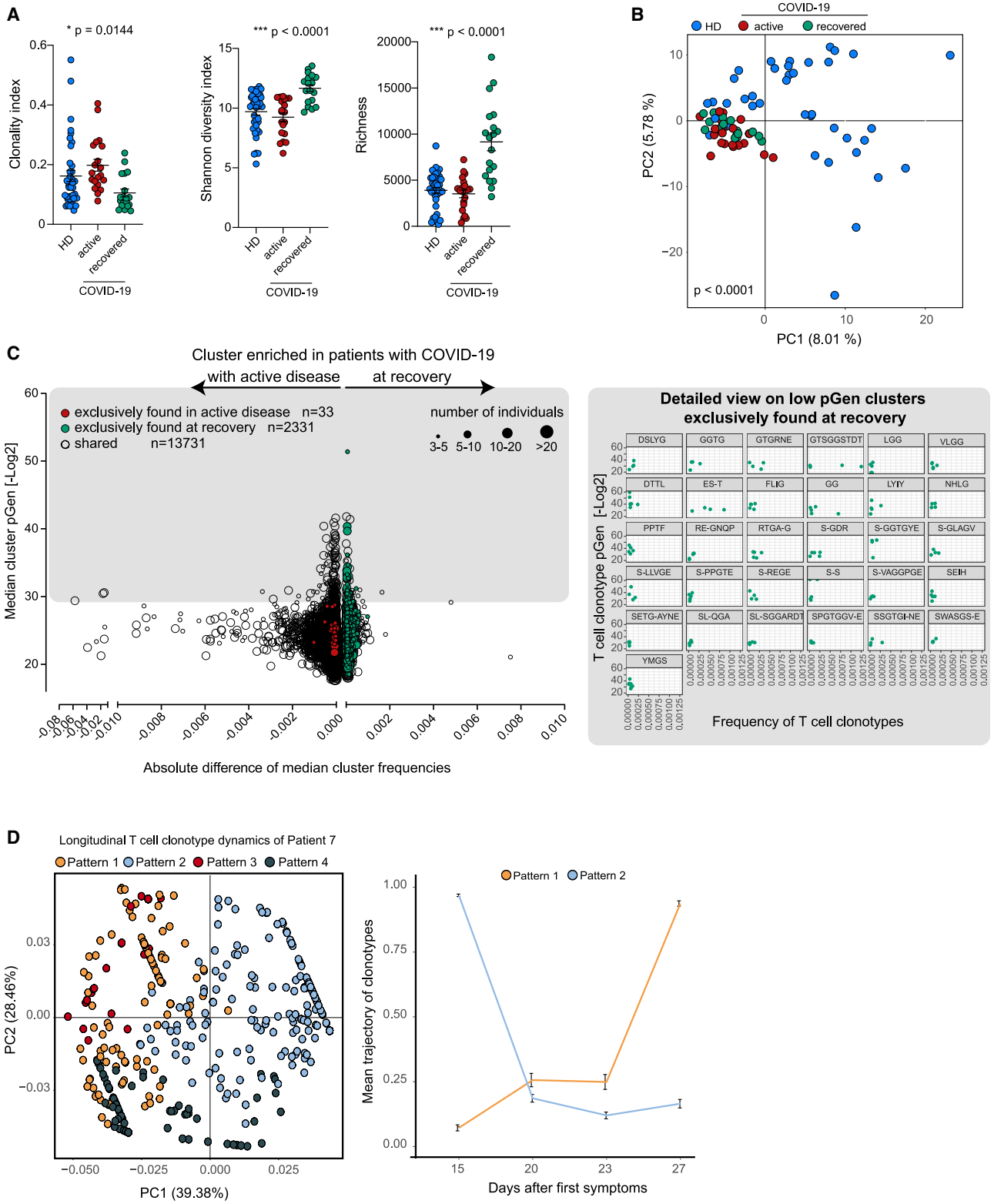

Figure 6. T Cell Repertoire Analysis from Living COVID-19 Sequence Repository Shows COVID-19-Specific, Shared TCR Clusters with Characteristic Clonotype Trajectories over Time

(A) Peripheral blood TRB repertoire metrics of HDs and patients with active COVID-19 and after recovery. The error bars indicate means ± SDs. Ordinary 1-way ANOVA was used to study differences between cohorts.

(legend continued on next page)

immune responses to SARS-CoV-2 had a larger pool of naive B cells. All of the COVID-19 cluster sequences are shown in detail in Table S5. Notably, we also detected 5 distinct B cell clonotypes in 8 different patients encoding BCRs very similar to an anti-SARS-CoV-2 single-domain antibody (n3010) recently isolated by Wu et al. (2020c) from a phage-displayed single-domain antibody library that was selected on the SARS-CoV-2 S1 antigen. These sequences also had a bias toward IGHV3 and IGHJ4 gene usage and exhibited low levels of somatic hypermutation with 98%–100% identity to the germline V gene (Figure 5D).

COVID-19-Specific T Cell Clusters Are Shared between Patients and Show Characteristic Clonotype Trajectories over the Course of the Disease

Global T cell metrics showed highly clonal T cell repertoires in active COVID-19, while, along with an overshooting T cell regeneration, T cell repertoires increased their diversity and richness above the level of HDs at recovery (Figure 6A). T cell receptor beta chain variable and joining (TRBV/J) gene usage was strongly skewed in patients with COVID-19 (Figure 6B). We used the GLIPH2 algorithm (grouping of lymphocyte interaction by paratope hotspots) to cluster TCR sequences based on presumed identical antigen recognition. In addition, we calculated the generation probability (pGen) of all T cell clonotypes contained in the clusters. T cell clonotypes with a high pGen, also called public clonotypes, are expected to be shared by >60% of the population due to their convergent recombination (Elhanati et al., 2018), while low pGen clusters are thought to be private and not expected in a large proportion of the population. Consequently, if low pGen sequences or clusters are shared between several individuals, it can be assumed that they were generated or selected during a directed immune response to a specific (e.g., infectious) trigger. The GLIPH2 algorithm was applied on all of the repertoires from cohorts 1 and 2. Clusters exclusively present or enriched at active (and mostly severe) disease contained predominantly public clonotypes (Figure 6C, left panel, lower left quadrant, and red dots), while only a few low pGen clusters were found to be enriched (Figure 6C, left panel, upper left quadrant). In contrast, we detected a high number of clusters exclusive to the recovered cohort 1 (n = 2,331; Figure 6C, left panel, green dots), including 31 low pGen clusters. Notably, the cluster with the lowest pGen of 2^{-51} and the sequence motif "S-GGTGYE" (Figure 6C, right panel) was shared exclusively by 3 patients at recovery (patients 6, 27, and 38). All of the relevant clusters, including their originating CDR3 amino acid sequence and their TRBV and TRBJ gene usage, are shown in Table S6.

Patient 7 developed only mild disease and successfully coped with the SARS-CoV-2 infection. Longitudinal sampling of this patient during active disease (days 15, 20, and 23) and at recovery (day 27) enabled us to dissect T cell dynamics during viral clearance. We analyzed the top 1,000 TCR clonotypes of this patient over all of the time points and identified 4 different patterns of clonotype dynamics by hierarchical clustering (Figure 6D, left panel). Patterns 1 and 2 especially caught our attention, since large numbers of clonotypes were assigned to them. The clonotypes of patterns 1 and 2 presented opposing trajectories, with pattern 2 clonotypes decreasing in frequency from day 20 until recovery and pattern 1 clonotypes constantly expanded over time, with the highest abundance at recovery (Figure 6D, right panel). We reasoned that if the expanding clonotypes of pattern 1 were crucial for the immune response during SARS-CoV-2 infection, they should also be included in the COVID-19-specific clusters shared between patients. Some of the expanding pattern 1 clonotypes derived from patient 7 were assigned to these clusters (e.g., to 10 COVID-19 clusters shared exclusively between recovered patients; cluster motifs: PNTGE, TGTGE, G-GGET, RG-PYNE, RQ-STDT, RTS-YNE, GLAGET, QAGANV, L-SGANV, and S-VGTGTYE).

DISCUSSION

We are in the early phase of a pandemic caused by the zoonotic SARS-CoV-2. Even if some of the immunological and inflammatory features of SARS-CoV or MERS-CoV may be similar for SARS-CoV-2, many of the vital questions remain unanswered. Most important, we have not deciphered adaptive immune responses in COVID-19 thus far. The first clinical data suggest that SARS-CoV-2 has a dramatic impact on cells of the adaptive immune system, but not all virus-induced immune reactions appear to be protective (Iwasaki and Yang, 2020; Jaume et al., 2011; Ko et al., 2017; Lee et al., 2006; Mehta et al., 2020; Merad and Martin, 2020; Tan et al., 2020; Wu et al., 2020b). Therefore, a more profound insight into the nature of beneficial versus detrimental B and T cell responses is critically needed. On the one hand, this will facilitate better prognostication in patients with risk factors and improve the monitoring of immunity to SARS-CoV-2 in recovered individuals. On the other hand, this knowledge may be used to enhance treatment (e.g., by cloning therapeutic monoclonal antibodies derived from immune repertoires of recovered patients) and, most important, to determine the optimal T cell engagement strategies for vaccines.

In the work presented here, we provide a comprehensive immunological profile of 2 cohorts of patients: cohort 1, comprising individuals recovered after mild to moderate COVID-19 disease, and cohort 2, comprising individuals with active infection and mostly severe disease courses. We show that almost all of the individuals with COVID-19 or a history of COVID-19 developed antibodies to SARS-CoV-2, including patients with major disturbances in B cell/Ig levels at active disease, including high IgA and normal or low IgG and IgM amounts as well as B lymphocytosis. The T cell pools of patients with active disease were considerably diminished and showed shifts toward $CD4^+$ and expanded Treg cells. We showed increased

(B) PCA of combinatorial TRBV/TRBJ gene usage in HDs and patients with active COVID-19 and after recovery. The statistical analysis was performed using the Pillai-Bartlett test of multivariate analysis of variance (MANOVA) of principal components 1 and 2.
(C) Distribution and pGen of COVID-19-specific T cell clusters in patients with active COVID-19 and after recovery.
(D) Principal-components analysis (PCA) of normalized clonotype frequencies of the most abundant 1,000 clonotypes over all time points (left panel). Mean trajectory ± SE of clonotypes belonging to pattern 1 (expanding) or pattern 2 (contracting) (right panel).
See also Figure S4 and Tables S3 and S6.

Th17 and Tfh and a trend toward non-classical Th1* cell responses, while a conventional Th1 cell response was not observed. The previously described antiviral immune activation or counterregulation patterns in both $CD4^+$ and $CD8^+$ T cell subsets were confirmed, and relevant checkpoints such as BTLA and CD73 were identified. The inhibitory checkpoints described on the cellular level were also mirrored by the level of soluble immune checkpoint molecules in our dataset (Diao et al., 2020; Zheng et al., 2020). In recovered patients, the soluble immune checkpoint molecules had returned to normal concentrations.

Moreover, our study confirms previously published data on the dysregulation of cytokines such as IL-6, IL-8, IL-10, IFN-γ-induced protein 10 (IP-10), tumor necrosis factor α (TNF-α), sCD25 (IL-2Ra), and IFN-γ (Chen et al., 2020; Diao et al., 2020; Hou et al., 2020). In addition to that, we show that IFN-β and IL-1β are increased in active COVID-19, which has not been found by others (Chen et al., 2020; Merad and Martin, 2020). In our view, a major strength of this comprehensive cytokine analysis is the demonstration of striking abnormalities in patients who have recovered from COVID-19 (some several weeks before the sampling time point), which to the best of our knowledge has only been investigated for a few selected cytokines thus far (Diao et al., 2020; Hou et al., 2020). We found a pronounced deregulation in cytokines and soluble factors exclusively increased at recovery (IL-12, APRIL, and sCD40L), while others were elevated independently of the disease state (TNF-β, IFN-γ1, IFN-α2, and IFN-γ2/3). The decreased amounts of IL-13 both in active disease and recovery are noteworthy, since this cytokine is involved in humoral immune reactions and alternative activation of macrophages, resulting in the release of anti-inflammatory stimuli (Gordon, 2003; Tangye et al., 2002). Also, the elevated levels of APRIL may be interesting since APRIL is known to support long-lived plasma cells in its niches (O'Connor et al., 2004). In the B cell context, the strong correlation of soluble BAFF levels with disease activity especially caught our attention. BAFF is an essential homeostatic cytokine for B cells that regulates splenic B cell numbers. Under physiological conditions, soluble BAFF shows a strict negative correlation with peripheral blood B cell numbers (Kreuzaler et al., 2012). Here, we found (1) a lack of B lymphopenia, with some patients even experiencing high B cell counts (unexpected in light of the pronounced T lymphopenia), and (2) a positive correlation of BAFF levels with B cell numbers. A possible explanation for this observation is the upregulation of BAFF triggered by the inflammatory environment of COVID-19. Typical BAFF producers are innate immune cells such as neutrophils that release BAFF in response to IFN stimulation or TLR ligation (Mackay and Schneider, 2009; Sjöstrand et al., 2016). In COVID-19, neutrophil counts are increased and IFN stimulation is part of the inflammatory reaction. Given the positive correlation between BAFF levels and B cell count in COVID-19, it seems plausible that B cell counts are driven by neutrophil granulocyte-produced BAFF. Another interesting aspect is the elevated levels of sCD40L in patients who have recovered from COVID-19. sCD40L can be shed from activated T cells, but it is also contained in platelet granules, and thus a well-known biomarker for platelet activation (Aloui et al., 2014). This is remarkable since patients with COVID-19 have an increased risk of thromboembolic events, and the finding of elevated sCD40L—in some patients several weeks after recovery—could raise concerns that this disease may increase cardiovascular risk over a longer time than suspected.

The most salient part of our study, however, is the examination of >14 million TCR and BCR sequences from the blood of COVID-19 patients and especially their clustering, enabling us to deduce COVID-19-relevant TCR or BCR signatures. Next-generation sequencing (NGS)-based analysis of TCR and BCR repertoires is an emerging technology that allows system-wide deciphering of the contribution of specific receptor configurations to adaptive immunity in infection, autoimmunity, or cancer. Sophisticated bioinformatic pipelines may permit a reduction of the complexity of the large datasets resulting from such trials to effectively discover reactive clusters of TCR and target specific BCR-antibody sequences.

Here, we aimed at clustering T cells relevant for immunity against SARS-CoV-2. We searched for TCR rearrangements with presumed shared antigen specificity, fulfilling the following requirements: (1) cluster of rearrangements of at least 4 different clonotype species with global and/or local paratope similarity, (2) low cluster-pGen, and (3) reduction of clusters present in HDs. Using this approach, we found 150 clusters with low pGen in COVID-19 patients that are likely of pathophysiological relevance. From this set, 31 clusters emerged as the most promising candidates associated with protective immunity due to their low pGen and selective occurrence in recovered individuals. The longitudinal monitoring of T cell repertoires derived from patient 7 during active disease and recovery was of particular importance, since we could identify clonotypes that expanded during the patient's successful immune response towards SARS-CoV-2, a pattern also found in two SARS-CoV-2 infected individuals with mild disease (Minervina et al., 2020). Notably, these clonotypes encompassed amino acid motifs that were also shared by other patients at recovery. Prospective studies will need to clarify whether the early expansion of such (preexisting) clonotypes affects the clinical course of COVID-19. Of note, we found that T cell repertoires of patients with a mild clinical course who recovered from COVID-19 were highly diverse. This could point to the direction that the ability to achieve effective TCR diversification may determine the chances of improved outcome and immune control in COVID-19, as suggested for other infections in mice and humans (Gil et al., 2015; Messaoudi et al., 2002; Price et al., 2004; Speranza et al., 2018).

While TCR clusters are essentially defined by paratope similarity, the shaping of B cell immune repertoires by antigens is more complex and not solely based on the expansion of clones with specific rearrangements. Most B cell responses essentially rely on maturation by somatic hypermutation in a germinal center reaction to produce clones with high BCR-antibody affinity. To detect BCR clusters likely targeting the same SARS-CoV-2 antigen, we clustered evolutionarily similar B cell clonotypes using phylogenetic trees. This analysis revealed a characteristic pattern of IGHV3 and IGHJ4/6 usage in clusters specific for antibody-positive individuals with COVID-19, suggesting that these sequences may correspond to those of SARS-CoV-2 antibodies. This was also supported by the identification of sequences with striking homology to antibody phage display clones selected on the SARS-CoV-2 S1 antigen (Wu et al., 2020c). The sequences within these clusters did not show substantial somatic hypermutation, suggesting that they represent naive responses. Also, we found that individuals with a more severe clinical course

(requiring mechanical ventilation/ECMO) had a significantly lower percentage of B lineage cells carrying an unmutated BCR, which is in line with previously published data by Nielsen et al. (2020). Although more detailed work on B lineage repertoire patterns is clearly needed, especially on samples acquired earlier in the disease course, these initial results may indicate that patients with B lineage repertoires exhibiting a high degree of somatic hypermutation may have a higher risk of a severe disease course and may require more stringent monitoring.

A potential mechanism of detrimental systemic effects of SARS-CoV-2 antibody responses can be conceived from our data in combination with the observations of Wu et al. (2020c), who isolated anti-SARS-CoV-2 single-domain antibodies. While these antibodies have been artificially selected on biopanned antigens, our data show that homologous sequences are also selected in humans, thereby validating these results. Wu et al. (2020c) showed that antibodies selected against the S1 domain of SARS-CoV-2 may be very diverse and may target a range of different epitopes, while only some are neutralizing. Our data may also point in this direction, since we found that the antibody response converged on different (and rather unmutated) IGHV3 rearrangements, while in none of our cases did a single dominant clone emerge in response to SARS-CoV-2. Of note, the phenomenon of a diverse range of neutralizing and non-neutralizing antibodies targeting different immunogenic S epitopes has not been observed in a similar way for SARS-CoV and MERS-CoV, in which a dominant antigenic loop makes it easy to isolate antibodies with neutralizing capacity (Wu et al., 2020c). One can speculate that diversification of the antibody response at the expense of protective antibodies may fuel the immunopathogenesis of COVID-19 via the antibody-dependent enhancement (ADE) of viral uptake. Among others, ADE is described in a macaque model of SARS-CoV, in which the presence of antibodies targeting the S protein causes enhanced S-IgG uptake by alveolar macrophages, resulting in functional polarization toward a proinflammatory phenotype with a lethal outcome due to acute lung injury (Liu et al., 2019). Detrimental effects of S-IgG have also been reported in mice (Tseng et al., 2012).

The B and T cell clusters reported here clearly require prospective validation to be used in different clinical settings. This could improve the diagnosis of asymptomatic patients and the identification of previously infected individuals and also help in estimating the risk of progression into more severe disease stages. Of note, T cells reactive to SARS-CoV-2 epitopes have been identified in individuals exposed to other ''common cold'' coronaviruses, suggesting some protective heterologous immunity (Grifoni et al., 2020), a concept that has also been proposed for cross-reactive antibodies induced in patients with SARS-CoV and MERS infections (Pinto et al., 2020). Our SARS-CoV-2 reactive TCR and BCR data may also help to define anti-SARS-CoV-2 immunity in individuals potentially pre-exposed to heterologous viruses on a population level.

Limitations of Study

One of the major limitations of this dataset is the paucity of available blood samples from COVID-19 patients with mild courses during the symptomatic phase of their disease and of early samples from patients with more severe courses. This material is difficult to obtain since patients with early disease or mild symptoms often isolate at home. However, it will be necessary to gather such samples to be able to validate the significance of our clusters for diagnosis in early disease. Another limitation of this study refers to the thus-far limited definition of protective versus detrimental adaptive immune responses and the prognostic significance of our clusters. A more stringent definition of protective responses will only be possible with earlier samples (as mentioned above), but also more longitudinal samples of patients recovering from COVID-19, sequencing of specific T cell subsets ($CD4^+$/Treg/$CD8^+$), and of sorted T cells responsive to SARS-2 peptide pools or of peptide-major histocompatibility complex (MHC)-$tetramer^+$ T cells. These experiments are ongoing and will likely deepen our understanding of SARS-CoV-2 immunity. Finally, while HLA typing has been performed on our patient cohort and data are provided in this article, we wish to point out that for an analysis of the contribution of certain HLA types to COVID-19 susceptibility or severity of disease, much larger datasets are clearly needed. This can only be achieved by collaborative efforts such as the COVID-HLA-GENOME (COHLAGE) project, which will also integrate sequence data from individual cohorts such as ours.

Our data clearly show the power of mining comprehensive immune repertoires for relevant immune cell clusters by using informative cohorts and potent clustering tools. In this way, the repository opened up for public scientific use will allow multiple researchers with different backgrounds to test their individual hypotheses on a growing dataset. Our living repository will expedite our understanding of prognostic immune response signatures across patients with COVID-19 to inform treatment benefits and even vaccine discovery for this pandemic disease. Ultimately, immune signature detection via NGS could flank existing serology-based tools for better diagnosis and monitoring.

STAR★METHODS

Detailed methods are provided in the online version of this paper and include the following:

- KEY RESOURCES TABLE
- RESOURCE AVAILABILITY
  - Lead Contact
  - Materials Availability
  - Data and Code Availability
- EXPERIMENTAL MODEL AND SUBJECT DETAILS
  - Patients and samples
  - Genomic HLA-typing
- METHOD DETAILS
  - ELISA determination of serostatus for SARS-CoV-2 IgG and IgA antibodies
  - Determination of SARS-CoV-2 neutralizing antibodies
  - Cytokine responses
  - T cell subset analysis by flow cytometry and data analysis
  - NGS immunosequencing and data analysis
- STATISTICAL ANALYSIS

SUPPLEMENTAL INFORMATION

Supplemental Information can be found online at https://doi.org/10.1016/j.immuni.2020.06.024.

ACKNOWLEDGMENTS

We thank the following investigators and advisors for contributing patients and samples, technical assistance, supporting lab facilities, biobanking, ethical, and other input: Nuray Akyuez, Samiya Al-Robaiy, Wolfgang Altermann, Herrmann Behre, Mildred Borrmann, Johanna Brandner, Christine Dierks, Jochen Dutzmann, Johann Fabian Eberhardt, Stephan Eisenmann, Lena Engels, Laura Glau, Katrin Hoffmann, Mareike Holz, Petra Hübner, Ulla Kasten-Pisula, Katharina Kolbe, Kerstin Körber-Fehrl, Katrin Lamszus, Beatrice Ludwig-Kraus, Cecile L. Maire, Sabine Matutat, Lutz P. Müller, Undine Musielinsky, Alexander Navarrete Santos and the FACS Core Facility Halle, Sebastian Nuding, Gerald Schlaf, Henning Seismann, Marta Siedlecki, Alexander Stein, Maria Vehreschild, Maxi Wass, Christoph Wosiek, Tanja Zeller, and Andela Zic. Moreover, we thank all of the patients and donors after recovery from COVID-19 for donating their blood for this project. This project was partially funded by the CRC 841 of the German Research Foundation (to M.B.) and by the Martin-Luther-University, Halle (Saale).

AUTHOR CONTRIBUTIONS

Idea & Design of Research Project, M.B., C.S., D.S., and L.P.; Supply of Critical Materials (e.g., patient material, cohorts, lab space, ethic advice, advice on work with infected material), D.G.S., M.B., C.S., L.v.W., I.W., M.A., and C.D.; Establishment of Methods, D.S., C.S., L.P., S.C., M.M., E.T., and E.W.; Experimental Work, C.S., L.P., D.S., R.S., and M.M.; Data Analysis & Interpretation, M.B., C.S., L.P., D.S., E.W., R.S., E.T., C.D., M.A., M.M., and S.C.; Drafting of Manuscript, M.B., C.S., L.P., D.S., L.v.W., R.S., E.T., and M.M.

DECLARATION OF INTERESTS

The authors declare no competing interests.

Received: May 27, 2020
Revised: June 19, 2020
Accepted: June 26, 2020
Published: June 30, 2020

REFERENCES

Aeffner, F., Woods, P.S., and Davis, I.C. (2015). Ecto-5′-nucleotidase CD73 modulates the innate immune response to influenza infection but is not required for development of influenza-induced acute lung injury. Am. J. Physiol. Lung Cell. Mol. Physiol. *309*, L1313–L1322.

Aloui, C., Prigent, A., Sut, C., Tariket, S., Hamzeh-Cognasse, H., Pozzetto, B., Richard, Y., Cognasse, F., Laradi, S., and Garraud, O. (2014). The signaling role of CD40 ligand in platelet biology and in platelet component transfusion. Int. J. Mol. Sci. *15*, 22342–22364.

Becattini, S., Latorre, D., Mele, F., Foglierini, M., De Gregorio, C., Cassotta, A., Fernandez, B., Kelderman, S., Schumacher, T.N., Corti, D., et al. (2015). T cell immunity. Functional heterogeneity of human memory CD4$^+$ T cell clones primed by pathogens or vaccines. Science *347*, 400–406.

Bolotin, D.A., Poslavsky, S., Mitrophanov, I., Shugay, M., Mamedov, I.Z., Putintseva, E.V., and Chudakov, D.M. (2015). MiXCR: software for comprehensive adaptive immunity profiling. Nat. Methods *12*, 380–381.

Brochet, X., Lefranc, M.-P., and Giudicelli, V. (2008). IMGT/V-QUEST: the highly customized and integrated system for IG and TR standardized V-J and V-D-J sequence analysis. Nucleic Acids Res. *36*, W503–W508.

Brüggemann, M., Kotrová, M., Knecht, H., Bartram, J., Boudjogrha, M., Bystry, V., Fazio, G., Froňková, E., Giraud, M., Grioni, A., et al.; EuroClonality-NGS Working Group (2019). Standardized next-generation sequencing of immunoglobulin and T-cell receptor gene recombinations for MRD marker identification in acute lymphoblastic leukaemia; a EuroClonality-NGS validation study. Leukemia *33*, 2241–2253.

Chen, G., Wu, D., Guo, W., Cao, Y., Huang, D., Wang, H., Wang, T., Zhang, X., Chen, H., Yu, H., et al. (2020). Clinical and immunological features of severe and moderate coronavirus disease 2019. J. Clin. Invest. *130*, 2620–2629.

Corrie, B.D., Marthandan, N., Zimonja, B., Jaglale, J., Zhou, Y., Barr, E., Knoetze, N., Breden, F.M.W., Christley, S., Scott, J.K., Cowell, L.G., and Breden, Felix (2018). iReceptor: A platform for querying and analyzing antibody/B-cell and T-cell receptor repertoire data across federated repositories. Immunological Reviews. https://doi.org/10.1111/imr.12666.

Diao, B., Wang, C., Tan, Y., Chen, X., Liu, Y., Ning, L., Chen, L., Li, M., Liu, Y., Wang, G., et al. (2020). Reduction and Functional Exhaustion of T Cells in Patients With Coronavirus Disease 2019 (COVID-19). Front. Immunol. *11*, 827.

Elhanati, Y., Sethna, Z., Callan, C.G., Jr., Mora, T., and Walczak, A.M. (2018). Predicting the spectrum of TCR repertoire sharing with a data-driven model of recombination. Immunol. Rev. *284*, 167–179.

Fuertes Marraco, S.A., Neubert, N.J., Verdeil, G., and Speiser, D.E. (2015). Inhibitory Receptors Beyond T Cell Exhaustion. Front. Immunol. *6*, 310.

Gautreau, G., Pejoski, D., Le Grand, R., Cosma, A., Beignon, A.-S., and Tchitchek, N. (2017). SPADEVizR: an R package for visualization, analysis and integration of SPADE results. Bioinformatics *33*, 779–781.

Gil, A., Yassai, M.B., Naumov, Y.N., and Selin, L.K. (2015). Narrowing of human influenza A virus-specific T cell receptor α and β repertoires with increasing age. J. Virol. *89*, 4102–4116.

Gordon, S. (2003). Alternative activation of macrophages. Nat. Rev. Immunol. *3*, 23–35.

Grifoni, A., Weiskopf, D., Ramirez, S.I., Mateus, J., Dan, J.M., Moderbacher, C.R., Rawlings, S.A., Sutherland, A., Premkumar, L., Jadi, R.S., et al. (2020). Targets of T Cell Responses to SARS-CoV-2 Coronavirus in Humans with COVID-19 Disease and Unexposed Individuals. Cell *181*, 1489–1501.

Han, M.V., and Zmasek, C.M. (2009). phyloXML: XML for evolutionary biology and comparative genomics. BMC Bioinformatics *10*, 356.

Hoffmann, M., Kleine-Weber, H., Schroeder, S., Krüger, N., Herrler, T., Erichsen, S., Schiergens, T.S., Herrler, G., Wu, N.-H., Nitsche, A., et al. (2020). SARS-CoV-2 Cell Entry Depends on ACE2 and TMPRSS2 and Is Blocked by a Clinically Proven Protease Inhibitor. Cell *181*, 271–280.e8.

Hou, H., Zhang, B., Huang, H., Luo, Y., Wu, S., Tang, G., Liu, W., Mao, L., Mao, L., Wang, F., et al. (2020). Using IL-2R/lymphocyte for predicting the clinical progression of patients with COVID-19. Clin. Exp. Immunol. *201*, 76–84.

Huang, H., Wang, C., Rubelt, F., Scriba, T.J., and Davis, M.M. (2020). Analyzing the Mycobacterium tuberculosis immune response by T-cell receptor clustering with GLIPH2 and genome-wide antigen screening. Nat. Biotechnol. https://doi.org/10.1038/s41587-020-0505-4.

Iwasaki, A., and Yang, Y. (2020). The potential danger of suboptimal antibody responses in COVID-19. Nat. Rev. Immunol. *20*, 339–341.

Jaume, M., Yip, M.S., Cheung, C.Y., Leung, H.L., Li, P.H., Kien, F., Dutry, I., Callendret, B., Escriou, N., Altmeyer, R., et al. (2011). Anti-severe acute respiratory syndrome coronavirus spike antibodies trigger infection of human immune cells via a pH- and cysteine protease-independent FcγR pathway. J. Virol. *85*, 10582–10597.

Ko, J.-H., Müller, M.A., Seok, H., Park, G.E., Lee, J.Y., Cho, S.Y., Ha, Y.E., Baek, J.Y., Kim, S.H., Kang, J.-M., et al. (2017). Serologic responses of 42 MERS-coronavirus-infected patients according to the disease severity. Diagn. Microbiol. Infect. Dis. *89*, 106–111.

Kreuzaler, M., Rauch, M., Salzer, U., Birmelin, J., Rizzi, M., Grimbacher, B., Plebani, A., Lougaris, V., Quinti, I., Thon, V., et al. (2012). Soluble BAFF levels inversely correlate with peripheral B cell numbers and the expression of BAFF receptors. J. Immunol. *188*, 497–503.

Lee, N., Chan, P.K.S., Ip, M., Wong, E., Ho, J., Ho, C., Cockram, C.S., and Hui, D.S. (2006). Anti-SARS-CoV IgG response in relation to disease severity of severe acute respiratory syndrome. J. Clin. Virol. *35*, 179–184.

Liu, L., Wei, Q., Lin, Q., Fang, J., Wang, H., Kwok, H., Tang, H., Nishiura, K., Peng, J., Tan, Z., et al. (2019). Anti-spike IgG causes severe acute lung injury by skewing macrophage responses during acute SARS-CoV infection. JCI Insight *4*, e123158.

Mackay, F., and Schneider, P. (2009). Cracking the BAFF code. Nat. Rev. Immunol. *9*, 491–502.

McKechnie, J.L., and Blish, C.A. (2020). The Innate Immune System: Fighting on the Front Lines or Fanning the Flames of COVID-19? Cell Host Microbe *27*, 863–869.

Mehta, P., McAuley, D.F., Brown, M., Sanchez, E., Tattersall, R.S., and Manson, J.J.; HLH Across Speciality Collaboration, UK (2020). COVID-19: consider cytokine storm syndromes and immunosuppression. Lancet *395*, 1033–1034.

Merad, M., and Martin, J.C. (2020). Pathological inflammation in patients with COVID-19: a key role for monocytes and macrophages. Nat. Rev. Immunol. *20*, 355–362.

Messaoudi, I., Guevara Patiño, J.A., Dyall, R., LeMaoult, J., and Nikolich-Zugich, J. (2002). Direct link between mhc polymorphism, T cell avidity, and diversity in immune defense. Science *298*, 1797–1800.

Minervina, A.A., Komech, E.A., Titov, A., Bensouda Koraichi, M., Rosati, E., Mamedov, I.Z., Franke, A., Efimov, G.A., Chudakov, D.M., Thierry, M., Walczak, A.M., Lebedev, Y.B., and Pogorelyy, M.V. (2020). Longitudinal high-throughput TCR repertoire profiling reveals the dynamics of T cell memory formation after mild COVID-19 infection. bioRxiv. In this issue. https://doi.org/10.1101/2020.05.18.100545.

Minervina, A.A., Pogorelyy, M.V., Komech, E.A., Karnaukhov, V.K., Bacher, P., Rosati, E., Franke, A., Chudakov, D.M., Mamedov, I.Z., Lebedev, Y.B., Mora, T., and Walczak, A.M. (2020). Primary and secondary anti-viral response captured by the dynamics and phenotype of individual T cell clones. eLife *9*, In this issue, e53704. In this issue. https://doi.org/10.7554/eLife.53704.

Nielsen, S.C.A., Yang, F., Hoh, R.A., Jackson, K.J.L., Roeltgen, K., Lee, J.-Y., Rustagi, A., Rogers, A.J., Powell, A.E., Kim, P.S., et al. (2020). B cell clonal expansion and convergent antibody responses to SARS-CoV-2. bioRxiv. https://doi.org/10.21203/rs.3.rs-27220/v1.

O'Connor, B.P., Raman, V.S., Erickson, L.D., Cook, W.J., Weaver, L.K., Ahonen, C., Lin, L.-L., Mantchev, G.T., Bram, R.J., and Noelle, R.J. (2004). BCMA is essential for the survival of long-lived bone marrow plasma cells. J. Exp. Med. *199*, 91–98.

Price, D.A., West, S.M., Betts, M.R., Ruff, L.E., Brenchley, J.M., Ambrozak, D.R., Edghill-Smith, Y., Kuroda, M.J., Bogdan, D., Kunstman, K., et al. (2004). T cell receptor recognition motifs govern immune escape patterns in acute SIV infection. Immunity *21*, 793–803.

Pinto, D., Park, Y.J., Beltramello, M., Walls, A.C., Tortorici, M.A., Bianchi, S., Jaconi, S., Culap, K., Zatta, F., De Marco, A., et al. (2020). Cross-neutralization of SARS-CoV-2 by a human monoclonal SARS-CoV antibody. Nature *583*, 290–295.

Price, M.N., Dehal, P.S., and Arkin, A.P. (2010). FastTree 2–approximately maximum-likelihood trees for large alignments. PLOS ONE *5*, e9490.

Puelles, V.G., Lütgehetmann, M., Lindenmeyer, M.T., Sperhake, J.P., Wong, M.N., Allweiss, L., Chilla, S., Heinemann, A., Wanner, N., Liu, S., et al. (2020). Multiorgan and Renal Tropism of SARS-CoV-2. N. Engl. J. Med. https://doi.org/10.1056/NEJMc2011400.

Rothe, C., Schunk, M., Sothmann, P., Bretzel, G., Froeschl, G., Wallrauch, C., Zimmer, T., Thiel, V., Janke, C., Guggemos, W., et al. (2020). Transmission of 2019-nCoV Infection from an Asymptomatic Contact in Germany. N. Engl. J. Med. *382*, 970–971.

Sallusto, F. (2016). Heterogeneity of Human CD4(+) T Cells Against Microbes. Annu. Rev. Immunol. *34*, 317–334.

Sethna, Z., Elhanati, Y., Callan, C.G., Walczak, A.M., and Mora, T. (2019). OLGA: fast computation of generation probabilities of B- and T-cell receptor amino acid sequences and motifs. Bioinformatics *35*, 2974–2981.

Shi, Y., Wang, Y., Shao, C., Huang, J., Gan, J., Huang, X., Bucci, E., Piacentini, M., Ippolito, G., and Melino, G. (2020). COVID-19 infection: the perspectives on immune responses. Cell Death Differ. *27*, 1451–1454.

Shubin, N.J., Chung, C.S., Heffernan, D.S., Irwin, L.R., Monaghan, S.F., and Ayala, A. (2012). BTLA expression contributes to septic morbidity and mortality by inducing innate inflammatory cell dysfunction. J. Leukoc. Biol. *92*, 593–603.

Simnica, D., Akyüz, N., Schliffke, S., Mohme, M., V Wenserski, L., Mährle, T., Fanchi, L.F., Lamszus, K., and Binder, M. (2019a). T cell receptor next-generation sequencing reveals cancer-associated repertoire metrics and reconstitution after chemotherapy in patients with hematological and solid tumors. OncoImmunology *8*, e1644110.

Simnica, D., Schliffke, S., Schultheiß, C., Bonzanni, N., Fanchi, L.F., Akyüz, N., Gösch, B., Casar, C., Thiele, B., Schlüter, J., et al. (2019b). High-Throughput Immunogenetics Reveals a Lack of Physiological T Cell Clusters in Patients With Autoimmune Cytopenias. Front. Immunol. *10*, 1897.

Sjöstrand, M., Johansson, A., Aqrawi, L., Olsson, T., Wahren-Herlenius, M., and Espinosa, A. (2016). The Expression of BAFF Is Controlled by IRF Transcription Factors. J. Immunol. *196*, 91–96.

Speranza, E., Ruibal, P., Port, J.R., Feng, F., Burkhardt, L., Grundhoff, A., Günther, S., Oestereich, L., Hiscox, J.A., Connor, J.H., and Muñoz-Fontela, C. (2018). T-Cell Receptor Diversity and the Control of T-Cell Homeostasis Mark Ebola Virus Disease Survival in Humans. J. Infect. Dis. *218* (*Suppl_5*), S508–S518.

Tan, W., Lu, Y., Zhang, J., Wang, J., Dan, Y., Tan, Z., He, X., Qian, C., Sun, Q., Hu, Q., et al. (2020). Viral Kinetics and Antibody Responses in Patients with COVID-19. medRxiv. https://doi.org/10.1101/2020.03.24.20042382.

Tangye, S.G., Ferguson, A., Avery, D.T., Ma, C.S., and Hodgkin, P.D. (2002). Isotype switching by human B cells is division-associated and regulated by cytokines. J. Immunol. *169*, 4298–4306.

Tseng, C.-T., Sbrana, E., Iwata-Yoshikawa, N., Newman, P.C., Garron, T., Atmar, R.L., Peters, C.J., and Couch, R.B. (2012). Immunization with SARS coronavirus vaccines leads to pulmonary immunopathology on challenge with the SARS virus. PLOS ONE *7*, e35421.

van Dongen, J.J.M., Langerak, A.W., Brüggemann, M., Evans, P.A.S., Hummel, M., Lavender, F.L., Delabesse, E., Davi, F., Schuuring, E., García-Sanz, R., et al. (2003). Design and standardization of PCR primers and protocols for detection of clonal immunoglobulin and T-cell receptor gene recombinations in suspect lymphoproliferations: report of the BIOMED-2 Concerted Action BMH4-CT98-3936. Leukemia *17*, 2257–2317.

VanDuijn, M.M., Dekker, L.J., van IJcken, W.F.J., Sillevis Smitt, P.A.E., and Luider, T.M. (2017). Immune Repertoire After Immunization As Seen by Next-Generation Sequencing and Proteomics. Frontiers in Immunology. In this issue. https://doi.org/10.3389/fimmu.2017.01286.

Walls, A.C., Park, Y.-J., Tortorici, M.A., Wall, A., McGuire, A.T., and Veesler, D. (2020). Structure, Function, and Antigenicity of the SARS-CoV-2 Spike Glycoprotein. Cell *181*, 281–292.e6.

Wang, D., Hu, B., Hu, C., Zhu, F., Liu, X., Zhang, J., Wang, B., Xiang, H., Cheng, Z., Xiong, Y., et al. (2020). Clinical Characteristics of 138 Hospitalized Patients With 2019 Novel Coronavirus-Infected Pneumonia in Wuhan, China. JAMA *323*, 1061–1069.

Wu, C., Chen, X., Cai, Y., Xia, J.a., Zhou, X., Xu, S., Huang, H., Zhang, L., Zhou, X., Du, C., et al. (2020a). Risk Factors Associated With Acute Respiratory Distress Syndrome and Death in Patients With Coronavirus Disease 2019 Pneumonia in Wuhan, China. JAMA Intern Med. e200994..

Wu, F., Wang, A., Liu, M., Wang, Q., Chen, J., Xia, S., Ling, Y., Zhang, Y., Xun, J., Lu, L., et al. (2020b). Neutralizing antibody responses to SARS-CoV-2 in a COVID-19 recovered patient cohort and their implications. medRxiv. https://doi.org/10.1101/2020.03.30.20047365.

Wu, Y., Li, C., Xia, S., Tian, X., Kong, Y., Wang, Z., Gu, C., Zhang, R., Tu, C., Xie, Y., et al. (2020c). Identification of Human Single-Domain Antibodies against SARS-CoV-2. Cell Host Microbe *27*, 891–898.e5.

Wu, Z., and McGoogan, J.M. (2020). Characteristics of and Important Lessons From the Coronavirus Disease 2019 (COVID-19) Outbreak in China: Summary of a Report of 72 314 Cases From the Chinese Center for Disease Control and Prevention. JAMA *323*, 1239–1242.

Zheng, H.-Y., Zhang, M., Yang, C.-X., Zhang, N., Wang, X.-C., Yang, X.-P., Dong, X.-Q., and Zheng, Y.-T. (2020). Elevated exhaustion levels and reduced functional diversity of T cells in peripheral blood may predict severe progression in COVID-19 patients. Cell. Mol. Immunol. *17*, 541–543.

Zhou, P., Yang, X.-L., Wang, X.-G., Hu, B., Zhang, L., Zhang, W., Si, H.-R., Zhu, Y., Li, B., Huang, C.-L., et al. (2020). A pneumonia outbreak associated with a new coronavirus of probable bat origin. Nature *579*, 270–273.

STAR★METHODS

KEY RESOURCES TABLE

REAGENT or RESOURCE	SOURCE	IDENTIFIER
Antibodies		
APC anti-PD-1 (Clone: EH12.2G7, Lot: B240811)	Biolegend (via Biozol, Munich, Germany)	Cat#329907
APC anti-CCR7 (Clone: G043H7, Lot: B274551)	Biolegend (via Biozol, Munich, Germany)	Cat#353245; RRID:AB_2750146
AlexaFluor700 anti-CD8 (Clone: RPA-T8, Lot: B253967)	Biolegend (via Biozol, Munich, Germany)	Cat# 344723; RRID:AB_629214
AlexaFluor488 anti-HLA-DR (Clone: L243, Lot: B246766)	Biolegend (via Biozol, Munich, Germany)	Cat#307619; RRID:AB_627944
FITC anti-2B4 (Clone: C1.7, Lot: B208362)	Biolegend (via Biozol, Munich, Germany)	Cat#329506; RRID:AB_1279186
FITC anti-Tgd (Clone: 11F2, Lot: 8005745)	BD Biosciences, USA	Cat#347903; RRID:AB_400358
PerCP-Cy5.5 anti-CD3 (Clone: UCHT1, Lot: B251283)	Biolegend (via Biozol, Munich, Germany)	Cat#560835; RRID:AB_2033956
PE-Cy7 anti-CD56 (Clone: 5.1H11, Lot: B256222)	Biolegend (via Biozol, Munich, Germany)	Cat#362509; RRID:AB_2563926
PE-Cy7 anti-CD39 (Clone: A1, Lot: B251864)	Biolegend (via Biozol, Munich, Germany)	Cat#328211; RRID:AB_2293623
PE-Cy7 anti-CCR4 (Clone: L291H4, Lot: B265812)	Biolegend (via Biozol, Munich, Germany)	Cat#359409; RRID:AB_2562430
PE-Dazzle anti-CXCR5 (Clone: J252D4, Lot: B226045)	Biolegend (via Biozol, Munich, Germany)	Cat#356903; RRID:AB_2561812
PE/Dazzle anti-TIGIT (Clone: A15153G, Lot: B254055)	Biolegend (via Biozol, Munich, Germany)	Cat#372724; RRID:AB_2715972
PE/Dazzle anti-CD28 (Clone: CD28.2, Lot: B242368)	Biolegend (via Biozol, Munich, Germany)	Cat#302941; RRID:AB_627002
PE anti-Tim-3 (Clone: F38-2E2, Lot: B260888)	Biolegend (via Biozol, Munich, Germany)	Cat#3153008; RRID:AB_2687644
PE anti-CD73 (Clone: AD2, Lot: B248074)	Biolegend (via Biozol, Munich, Germany)	Cat#344003
PE anti-CCR6 (Clone: G034E3, Lot: B240450)	Biolegend (via Biozol, Munich, Germany)	Cat#3141003A; RRID:AB_2687639
BV421 anti-CRTH2 (Clone: BM16, Lot: B245754)	Biolegend (via Biozol, Munich, Germany)	Cat#350111; RRID:AB_2112695
BV421 anti-CD25 (Clone: BC96, Lot: B261190)	Biolegend (via Biozol, Munich, Germany)	Cat#302629; RRID:AB_626993
BV421 anti-BTLA (Clone: MIH26, Lot: B238296)	Biolegend (via Biozol, Munich, Germany)	Cat#344511; RRID:AB_2065765
BV5218(BV510) anti-CD4 (Clone: RPA-T4, Lot: B249258)	Biolegend (via Biozol, Munich, Germany)	RRID:AB_629054
BV605 anti-CD27 (Clone: O323, Lot: B241914)	Biolegend (via Biozol, Munich, Germany)	Cat#302829; RRID:AB_629018
BV605 anti-CD161 (Clone: HP3G10, Lot: B245750)	Biolegend (via Biozol, Munich, Germany)	Cat#339915
BV605 anti-CD57 (Clone: QA17A04, Lot: B276635)	Biolegend (via Biozol, Munich, Germany)	Cat#393305; RRID:AB_2734459
BV650 anti-CD127 (Clone: A019D5, Lot: B257518)	Biolegend (via Biozol, Munich, Germany)	Cat#351352; RRID:AB_2734366
BV650 anti-CXCR3 (Clone: G025H7, Lot: B225762)	Biolegend (via Biozol, Munich, Germany)	Cat#3156004B; RRID:AB_2687646
BV711 anti-KLRG1 (Clone: 2F1/KLRG1, Lot: B266677)	Biolegend (via Biozol, Munich, Germany)	Cat#138407; RRID:AB_10574005

(*Continued on next page*)

Continued

REAGENT or RESOURCE	SOURCE	IDENTIFIER
BV785 anti-CD45RA (Clone: HI100, Lot: B246562)	Biolegend (via Biozol, Munich, Germany)	Cat#304139; RRID:AB_10705799
BV785 anti-CD25 (Clone: BC96, Lot: B237289)	Biolegend (via Biozol, Munich, Germany)	Cat#302637; RRID:AB_626993
Bacterial and Virus Strains		
SARS-CoV-2 FFM1 isolate	was isolated from a patient at University Hospital Frankfurt who was tested positive for SARS-CoV-2 by PCR	N/A
Biological Samples		
Peripheral blood of patients with active COVID-19 disease and after recovery	This paper	N/A
Chemicals, Peptides, and Recombinant Proteins		
Phusion HS II	Thermo Fisher Scientific, Darmstadt, Germany	Cat#F549S
Critical Commercial Assays		
Anti-SARS-CoV-2-ELISA IgA	Euroimmun AG, Lübeck, Germany	Cat#EI 2606-9601 A
Anti-SARS-CoV-2-ELISA IgG	Euroimmun AG, Lübeck, Germany	Cat#EI 2606-9601 G
LEGENDplex Human B Cell Panel (13-plex)	BioLegend (via Biozol, Munich, Germany)	Cat#740527
Human Immune Checkpoint Panel 1 (10-plex)	BioLegend (via Biozol, Munich, Germany)	Cat#740962
Human Anti-Virus Response Panel (13-plex)	BioLegend (via Biozol, Munich, Germany)	Cat#740390
Deposited Data		
NGS Sequencing annotated data	iReceptor Public Archive	ID IR-Binder-000001
NGS Sequencing fastq data	European Nucleotide Archive	ID PRJEB38339
Experimental Models: Cell Lines		
Caco-2 cells	ATCC DSMZ	Cat# ACC-169: RRID:CVCL_0025
Oligonucleotides		
BIOMED2-FR1 (IGH)	(van Dongen et al., 2003)	N/A
BIOMED2-TRB-A/ B	(van Dongen et al., 2003)	N/A
Software and Algorithms		
R Studio version 3.5.1	RStudio, Boston, USA	https://rstudio.com/products/rstudio/
GraphPad Prism 8.0.2	GraphPad Software, La Jolla, CA, USA	https://www.graphpad.com/scientific-software/prism/
FlowJo v10	BD, USA	https://www.flowjo.com/solutions/flowjo
SPADEVizR	(Gautreau et al., 2017)	https://rdrr.io/github/tchitchek-lab/SPADEVizR/
MiXCR (3.0.8)	(Bolotin et al., 2015)	https://mixcr.readthedocs.io/en/master/
IMGT/HighV-QUEST	Brochet et al., 2008	http://www.imgt.org/HighV-QUEST/home.action
OLGA	Sethna et al., 2019	https://github.com/statbiophys/OLGA
GLIPH2	Huang et al., 2020	http://50.255.35.37:8080/
FastTreeMP	Price et al., 2010	http://www.microbesonline.org/fasttree/
Archaeopteryx viewer (0.9928 beta)	Han and Zmasek, 2009	https://sites.google.com/site/cmzmasek/home/software/archaeopteryx

RESOURCE AVAILABILITY

Lead Contact

Further information and requests for resources and reagents should be directed to and will be fulfilled by the Lead Contact, Mascha Binder (mascha.binder@uk-halle.de).

Materials Availability

This study did not generate new unique reagents.

Data and Code Availability

From the iReceptor Public Archive (IPA) our data will be findable as part of the AIRR Data Commons using the iReceptor Gateway (Corrie et al., 2018) (https://gateway.ireceptor.org; iReceptor Study ID IR-Binder-000001). Moreover, we have deposited our raw fastq sequencing files in the European Nucleotide Archive with the accession number ENA: PRJEB38339.

EXPERIMENTAL MODEL AND SUBJECT DETAILS

Patients and samples

We focused our investigation on two sets of patients: Cohort 1 included recovered individuals, the majority after mildly symptomatic COVID-19 disease. Cohort 2 had been assembled at the University Medical Centers Halle and Frankfurt. This cohort included patients with severely symptomatic COVID-19 disease, all of which requiring hospitalization. Up to 9 follow-up blood samples were available per patient, some of which spanning different disease stages in the same patient. Age-matched healthy donors (n = 39) were used as a reference. Patient characteristics are summarized in Table S1. Blood collection was performed under institutional review board approvals number 2020-039 and 11/17.

Genomic HLA-typing

All patients were genotyped through the use of sequence-specific primer- (SSP-) PCR-based low resolution technique (Innotrain, Kronberg, Germany and in some cases, additionally, Protrans. Ketsch, Germany) both for HLA class I loci A, B and C (Cw) and for the HLA class II loci DRB1* (DR), DRB3* (DR52), DRB4* (DR53), DRB5* (DR51) and DQB1* (DQ).

METHOD DETAILS

ELISA determination of serostatus for SARS-CoV-2 IgG and IgA antibodies

Plasma levels of anti-SARS-CoV-2 antibodies was determined using the Anti-SARS-CoV-2-ELISA IgA and IgG (Euroimmun AG, Lübeck, Germany) according to the manufactureŕs instructions. The kit employs a recombinant S1 domain of the SARS-CoV-2 spike (S) protein as antigen. Readouts were performed at 450 nm using a Tecan Spectrophotometer SpectraFluor Plus (Tecan Group Ltd., Männedorf, Switzerland).

Determination of SARS-CoV-2 neutralizing antibodies

To test for neutralizing capacity of SARS-CoV-2 specific antibodies, Caco-2 cells (human colon carcinoma cells, ATCC DSMZ ACC-169 (American Type Culture Collection, Manassas, Virginia, USA)) were seeded on a 96-well plate 3-5 days prior infection. 2-fold dilutions of the test sera beginning with a 1:10 dilution (1:10; 1:20; 1:40; 1:80; 1:160; 1:320; 1:640 and 1:1280) were made in culture medium (Minimum essential medium, MEM; GIBCO, Dublin, Ireland) before mixed 1:1 with 100 TCID50 (Tissue culture infectious dose 50) of reference virus (SARS-CoV-2 FFM1 isolate). FFM1 was isolated from a patient at University Hospital Frankfurt who was tested positive for SARS-CoV-2 by PCR. Virus-serum mixture was incubated for one hour at 37°C and transferred onto the cell monolayer. Virus related cytopathic effects (CPE) were determined microscopically 48 to 72 h post infection. To determine a potential neutralizing ability of patient serum, CPE at a sample dilution of 1:10 is defined as non-protective while a CPE at a dilution of > 1:20, is defined as protective.

Cytokine responses

Plasma was isolated by centrifugation of whole blood for 15 minutes at 2000 x g. Samples were stored at - 80°C before use. Cytokine plasma levels were detected using the LEGENDplex Human B Cell Panel (13-plex), Human Immune Checkpoint Panel 1 (10-plex) and the Human Anti-Virus Response Panel (13-plex) BioLegend (via Biozol, Munich, Germany) according to the supplier's suggestions. Data was acquired using the BD FACSCelesta flow cytometer and analyzed with the BioLegend LEGENDplex software.

T cell subset analysis by flow cytometry and data analysis

In brief, PBMCs, frozen in fetal bovine serum + 10% DMSO, were defrosted and incubated with three different multicolor antibody panels for 45min at room temperature in the dark, after FC blocking was performed. Cells were washed and fixed in 4% PFA for 50min at room temperature in the dark before the analysis was performed. Cells were measured with an LSRFortessa (BD Biosciences). Following antibodies were used: APC anti-PD-1 (Clone: EH12.2G7, Lot: B240811, Biolegend), APC anti-CCR7 (Clone: G043H7, Lot: B274551, Biolegend), AlexaFluor700 anti-CD8 (Clone: RPA-T8, Lot: B253967, Biolegend), AlexaFluor488 anti-HLA-DR (Clone: L243, Lot: B246766, Biolegend), FITC anti-2B4 (Clone: C1.7, Lot: B208362, Biolegend), FITC anti-Tgd (Clone: 11F2, Lot: 8005745, BD Biosciences), PerCP-Cy5.5 anti-CD3 (Clone: UCHT1, Lot: B251283, Biolegend), PE-Cy7 anti-CD56 (Clone: 5.1H11, Lot: B256222, Biolegend), PE-Cy7 anti-CD39 (Clone: A1, Lot: B251864, Biolegend), PE-Cy7 anti-CCR4 (Clone: L291H4, Lot: B265812, Biolegend), PE-Dazzle anti-CXCR5 (Clone: J252D4, Lot: B226045, Biolegend), PE/Dazzle anti-TIGIT (Clone: A15153G, Lot: B254055, Biolegend), PE/Dazzle anti-CD28 (Clone: CD28.2, Lot: B242368, Biolegend), PE anti-Tim-3 (Clone: F38-2E2, Lot:

B260888, Biolegend), PE anti-CD73 (Clone: AD2, Lot: B248074, Biolegend), PE anti-CCR6 (Clone: G034E3, Lot: B240450, Biolegend), BV421 anti-CRTH2 (Clone: BM16, Lot: B245754, Biolegend), BV421 anti-CD25 (Clone: BC96, Lot: B261190, Biolegend), BV421 anti-BTLA (Clone: MIH26, Lot: B238296, Biolegend), BV5218(BV510) anti-CD4 (Clone: RPA-T4, Lot: B249258, Biolegend), BV605 anti-CD27 (Clone: O323, Lot: B241914, Biolegend), BV605 anti-CD161 (Clone: HP3G10, Lot: B245750, Biolegend), BV605 anti-CD57 (Clone: QA17A04, Lot: B276635, Biolegend), BV650 anti-CD127 (Clone: A019D5, Lot: B257518, Biolegend), BV650 anti-CXCR3 (Clone: G025H7, Lot: B225762, Biolegend), BV711 anti-KLRG1 (Clone: 2F1/KLRG1, Lot: B266677, Biolegend), BV785 anti-CD45RA (Clone: HI100, Lot: B246562, Biolegend), BV785 anti-CD25 (Clone: BC96, Lot: B237289, Biolegend). Manual data analysis by classical hierarchical gating was performed using BD FACS Diva and FlowJo v10 software (BD, USA). SPADEVizR(Gautreau et al., 2017) was used for unsupervised clustering and differential expression analysis of the flow cytometry raw data, while UMAP embedding was used for dimensionality reduction and visualization of the manually analyzed data.

NGS immunosequencing and data analysis

To determine the entirety of the clonal V(D)J rearrangements of peripheral T and B cell receptors (T / B cell repertoire), all acquired blood samples underwent next-generation sequencing of the *TRB* and *IGH* genetic locus. In brief, genetic loci were amplified together in a multiplex PCR using BIOMED2-FR1 (*IGH*) or *–TRB-A/ B* primer pools and 250–500 ng of genomic DNA (Brüggemann et al., 2019; van Dongen et al., 2003). The primers were purchased from Metabion International AG (Martinsried, Germany). Two consecutive PCR reactions were performed to generate fragments tagged with Illumina-compatible adapters for hybridization to the flow cell and 7 nucleotide barcodes for sample identification. All PCRs were performed using Phusion HS II (Thermo Fisher Scientific Inc., Darmstadt, Germany). After gelelectrophoretic separation, amplicons were purified using the NucleoSpin® Gel and PCR Clean-up kit (Macherey-Nagel, Düren, Germany), quantified on the Qubit platform (QIAGEN, Hilden, Germany) and pooled to a final concentration of 4 nM. The quality of the amplicon pools was controlled on an Agilent 2100 Bioanalyzer (Agilent Technologies, Böblingen, Germany) before undergoing NGS. Annotation of *TRB* and *IGH* loci rearrangements was computed with the MiXCR framework (3.0.8) (Bolotin et al., 2015). As reference for sequence alignment the default MiXCR library was used for *TRB* sequences and the IMGT library v3 for *IGH*. Non-productive reads and sequences with less than 2 read counts were not considered for further analysis. Each unique complementarity-determining region 3 (CDR3) nucleotide sequence was defined as one clone. All analyses and data plotting was performed using R version 3.5.1. Broad repertoire metrics (clonality, diversity, richness), somatic hypermutation (*IGH*) and V(-J) gene usage were analyzed and plotted as previously described (Simnica et al., 2019a, 2019b).

Further, presumably virus-specific TCR and BCR (or neutralizing antibody sequences) were bioinformatically deduced by comparing immune repertoires of COVID-19 patients with corresponding control groups (healthy donors and an Ebola vaccination cohort; Table S4). As previously described by our group (Simnica et al., 2019a, 2019b), we used the established cluster algorithm GLIPH2 (grouping of lymphocyte interactions by paratope hotspots) (Huang et al., 2020) for clustering of T cells by global and/or local similarity of the CDR3 amino acid sequence flanked by the calculation of generation probability (pGen) using OLGA (Optimized Likelihood estimate of immunoGlobulin Amino-acid sequences) (Sethna et al., 2019). To exclude contamination bias (which might have occurred during sequencing and/or sample preparation) we chose a stringent threshold and only included clusters in our analysis, which contained a minimum of four unique TCR clonotypes and were present at least in three individuals. The median pGen is shown for each cluster and is transformed to Log2 for plotting purposes. The frequency of each cluster is represented by the median frequency of all clonotypes it consists of.

Over time dynamics of the 1000 most abundant clonotypes were plotted following the general approach published by Minervina et al., 2020a, 2020b for patient 7 who had mild disease and several follow-up samples until recovery. Briefly, the normalized clonotype frequency over the time course was used to generate an Euclidean distant matrix. Using hierarchical clustering, we identified four distinct patterns of clonotype dynamics. We generated a PCA based on the normalized clonotype trajectories, color-coded the four different patterns and plotted mean trajectories for the most dominant patterns 1 and 2.

Repertoire-wide evolutionary analysis of B cells was performed using approximately maximum-likelihood trees, a concept shown to successfully cluster B cell sequences in the context of immunization (VanDuijn et al., 2017). Briefly, the most abundant 50 clones of each repertoire were used for the analysis. Therefore, the nucleotide sequence of each clone (covering framework region (FR) 2 to CDR3 of the rearranged IGH locus) was converted into the according amino acid sequence and gapped according to the IMGT unique numbering using HighV-QUEST (Brochet et al., 2008). The resulting fasta files were used to infer phylogenetic trees with FastTreeMP (Price et al., 2010) and the data were visualized and analyzed using the Archaeopteryx viewer (0.9928 beta) (Han and Zmasek, 2009). We defined a relevant cluster to consist of at least 10 unique BCR clonotypes from at least 4 different patients.

STATISTICAL ANALYSIS

Differences in NGS metrics and cytokine levels were studied by ordinary one-way ANOVA and Student's t test. PCA differences by Pillai–Bartlett test of MANOVA. All statistical analyses were performed using R version 3.5.1 and GraphPad Prism 8.0.2 (GraphPad Software, La Jolla, CA, USA).